sciendo

ANNALS OF WEST UNIVERSITY OF TIMISOARA PHYSICS
Vol. LXIV, 2022

DOI : 10.2478/awutp-2022-0003

STRUCTURAL, ELECTRONIC, ELASTIC, MECHANICAL, OPTICAL AND THERMOELECTRIC PROPERTIES OF THE CHALCOGENIDE DOUBLE PEROVSKITES A_2GaNbS_6 (A = Ca, Sr AND Ba): INSIGHTS FROM DENSITY FUNCTIONAL THEORY CALCULATIONS

H. Bendjilali*, A. Chahed, H. Rozale, M.N. Bousahla and Y.A. Khachai

Condensed Matter and Sustainable Development Laboratory (LMCDD), University of Sidi Bel-Abbes, Sidi Bel-Abbes 22000, Algeria

**e-mail : hadjer.bendjilali@yahoo.com; hadjer.bendjilali@univ-sba.dz*

Article Info

Received : 07.03.2022
Accepted: 10.05.2022

Keywords :

DFT, Chalcogenide double perovskites, optoelectronic properties, thermoelectric properties

Abstract

Recently, the lead-free double perovskite compounds have been evinced to be promising candidate for thermoelectric and optoelectronic technologies. In this paper; we have probed a theoretical works on the different physical properties: Structural, electronic, elastic, optical and thermoelectrical properties of the chalcogenide double perovskites A_2GaNbS_6 (A=Ca, Sr and Ba) within the instructions of density functional theory. The calculations have incorporated using the full potential linearized augmented plane waves (FP-LAPW) method within gradient generalized approximation (GGA) and the modified Becke-Johnson potential (mBJ) to describe the exchange-correlation potential as embodied in the WIEN2K code. The computed structural results show that the non-magnetic structure state is energetically the most stable structure in the cubic $Fm\bar{3}m$ (225) configuration, also the elastic and mechanical properties indicate that A_2GaNbS_6 (A=Ca, Sr and Ba) have a ductile nature. According to the electronic plots the three compounds have a semiconducting behavior with indirect (pseudo-direct) band gap of 1.21, 1.28 and 1.32 eV. Important optical responses of studied chalcogenide double perovskites are found in the visible and ultraviolet energy ranges. Finally, the thermoelectric effectiveness of the three compounds have been probed by computing parameters like Seebeck coefficient, electrical conductivity, thermal conductivity and figure of merit with semi-classical Boltzmann theory and constant relaxation time approximation as implemented in BoltzTrap code, the obtained results show that the chalcogenide double perovskites could be a good candidate for thermoelectric applications.

1. Introduction

Latterly, the search for new multifunctional materials with high-efficiency optoelectronic and thermoelectric responses has been trigged the interests of the scientific community [1-4]. These types of materials are valuable for energy-conversion applications, which means transforming the waste heat into useful electricity for the thermoelectric materials and the abundant light to electricity for the photovoltaic materials, therefore, they are consequently proving to be environmentally friendly alternatives, and economical. Such as Skutterudites [5], the half-Heusler alloys [6,7], perovskites materials [8-10]. The general stoichiometric formula ABX_3 assort a vast family of compounds; the perovskites compounds, which A-constituent represents alkali/rare-earth metals, the element B is usually a transition-metal, while X represents a chalcogen [11] or halogen [12]. Because of their flexibility, the perovskites materials without difficulty permit change in composition to have higher physics output in optoelectronic, magnetic and thermoelectric properties. However, the addition another B' (transition-metal) element at the B-site means doubling of constituents allows for the possibility to form double perovskite $A_2BB'X_6$ [13]. They have been studied since 1960's [14-16]. Over 300 compounds with double perovskite structure have been synthesized [17-20]. Furthermore, the focus on double perovskites has drawn great interests due to their unique suitable properties such as ferromagnetism [21], half-metallic properties [22] and optical properties [23].

Agiorgousis et al. [24] evaluated some chalcogenide double perovskite compounds through machine learning and augmented discovery for photovoltaics such as Ba_2GaNbS_6 and Ca_2GaNbS_6. However, to our knowledge, no study has shown that these materials have been synthesized or studied by the ab-initio (DFT) calculations or even experimentally. Motivated by the above, our main aim in this manuscript is to provide theoretical guidance for future experiments, we investigated the structural, electronic, elastic, optical and thermoelectric properties in details of the three chalcogenide double perovskites compounds Ba_2GaNbS_6, Sr_2GaNbS_6 and Ca_2GaNbS_6 using first-principles (DFT) calculations.

2. Computational method

We have carried out density functional theory calculation (DFT) [25, 26] using the full potential linearized augmented plane wave formalism (FP-LAPW) as embodied in the WIEN2K code [27]. The correlation-exchange interaction energy and potential are approximated through the generalized gradient approximation of Perdew-Burke-Ernzehof

(PBE-GGA) [28, 29]. Also, we have used the modified Becke-Jonhson (mBJ) approach [30] to overcome the limitations of GGA. In the non-overlapping muffin-tin spheres, the wave function was expanded to $l_{max} = 10$ in the harmonic spherical basis set. In the interstitial regions, the wave function was expanded in a plane wave basis set with a cut-off parameter $R_{MT}K_{max} = 8$, where R_{MT} is the smallest muffin-tin radius and K_{max} refers to the largest K-vector in the first Brillouin zone. We set the muffin-sphere radius to 2.0, 2.2, 2.4 a.u for Ca, Sr, and Ba atoms and to 2.10, 2.15, and 1.90 a.u for Ga, Nb, and S atoms respectively. To separate the core states from valence ones, cut-off energy is set to be -6.0 Ry. The Brillouin zone integration is completed over a Monkhorst-Package [31, 32] with 12 × 12 × 12 k-mesh. The convergence criterion of the self-consistent total energy is taken to be 10-4 Ry. Similarly, the optical properties were calculated with 20 × 20 × 20 k-points. The dense k-mesh of 45 × 45 × 45 was used to obtain accurate thermoelectric properties, which are calculated with semi-classical Boltzmann theory and constant relaxation time approximation asset in Boltz Trap code [33], in addition to the rigid band approximation.

3. Results and discussion

3. 1. Structural properties

The structural properties of stable state of double perovskite materials can be determined by many factors like optimizing crystal structure utilizing an equation of state, and Goldschmidt's tolerance factor "*t*" [34]:

$$t = \frac{r_A + r_X}{\sqrt{2}(r_B + r_X)} \quad (1)$$

where r_A, r_B and r_X are the ionic radii of the atoms in the A, B, and X sites, respectively. The optimal tolerance factor range to form a perovskite is $0.71 < t < 1.0$; orthorhombic structures are preferred when $t < 0.9$ and cubic structures are preferred when $0.9 < t < 1.0$.

In the present case, the values of tolerance factor "*t*" are in the range of 0.9 to 1, the chalcogenide double perovskite compounds A_2GaNbS_6 (A=Ca, Sr and Ba) are stabilized in a cubic structure which is illustrated in Fig.1, with space group $Fm\bar{3}m$ (n°.225) in accordance to Hermann-Mauguin convention [35], with Ba, Sr and Ca atoms are situated at 8c (0.25, 0.25, 0.25), Ga at (0, 0, 0), Nb at 4b (0.5, 0.5, 0.5) and S at 24e (0.25, 0, 0) Wyckoff positions [36].The optimized structural parameters as shown in Fig. 2 of the chalcogenide double perovskites Ca_2GaNbS_6, Sr_2GaNbS_6, and Ba_2GaNbS_6 for non-magnetic (NM) and

ferromagnetic (FM) states are computed by utilizing the Murnaghan equation state [37], which justified the cubic stability with non-magnetic (NM) ground state because it has the lowest energy for the three compounds. All the results are cited in Table 1. No experimental or theoretical data are available in scientific literature for the structural properties to compare with it.

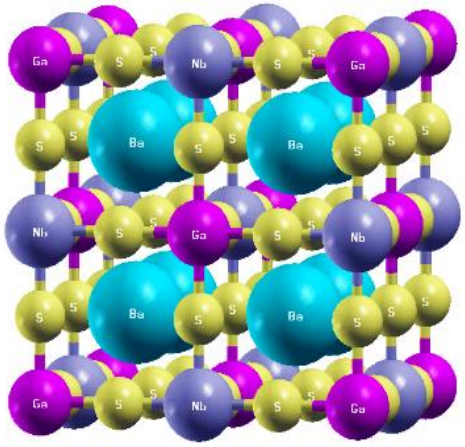


Figure 1. Crystal structure of the Ba_2GaNbS_6 double perovskite as prototype.

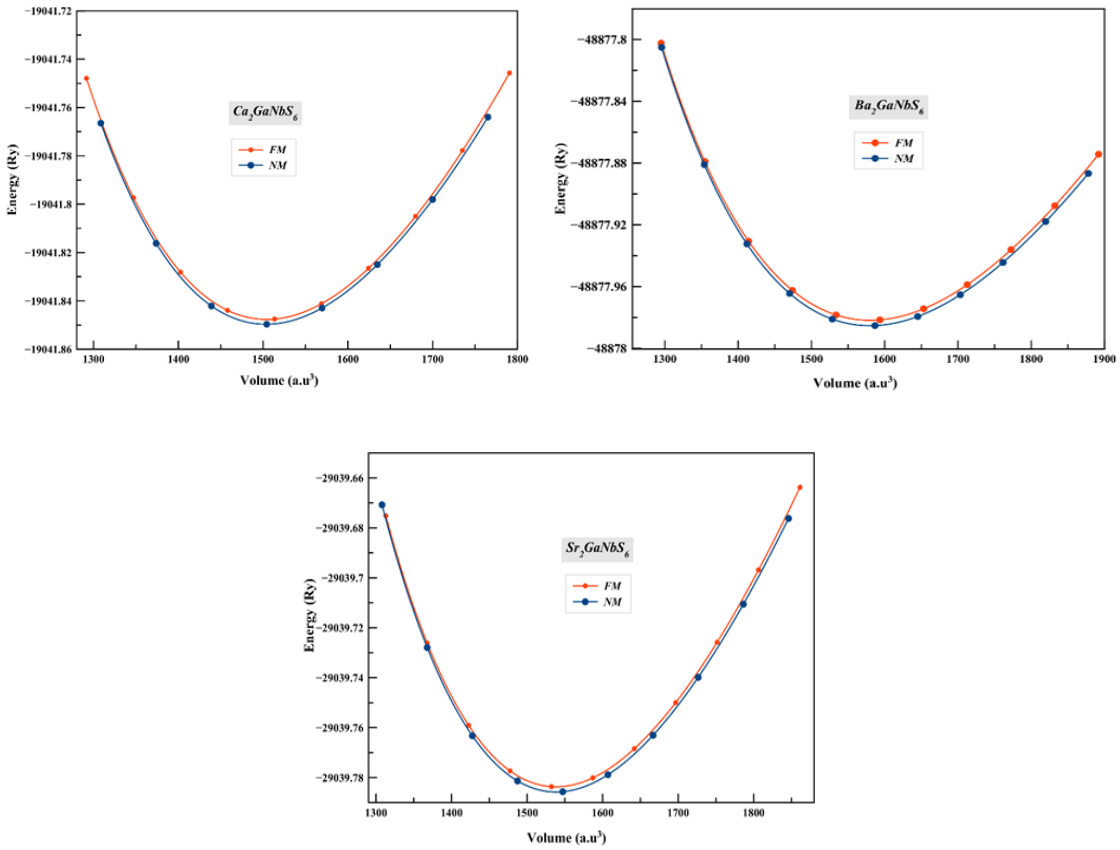


Figure 2. Optimization plots of A_2GaNbS_6 in non-magnetic (NM) and ferromagnetic (FM) phases using GGA approximation.

Table 1. Optimized parameters: Equilibrium lattice parameter a_0 (A°), Bulk modulus B (GPa), pressure derivative of bulk modulus B' and total energies E_0 (Ry) and Goldschmidt tolerance Factor (t) of the three double perovskites A_2GaNbS_6

Compound		GGA					*t*
		a_0(A°)	V_0(a.u^3)	B(GPa)	B'	E_0(Ry)	
Ba_2GaNbS_6	*NM*	9.7837	1579.9734	70.3201	4.5951	-48877.985256	0.987
	FM	9.7841	1580.1562	70.3351	4.4324	-48877.981752	
Sr_2GaNbS_6	*NM*	9.6972	1538.4024	72.0891	4.4671	-29039.785775	0.939
	FM	9.6969	1538.2670	72.1823	4.3515	-29039.783693	
Ca_2GaNbS_6	*NM*	9.6233	1503.5166	73.9720	4.6267	-19041.849665	0.910
	FM	9.6245	1504.0599	74.0526	4.3129	-19041.847669	

3. 2. Elastic and mechanical properties

The elastic properties of materials provide a necessary knowledge on their mechanical strength also the elastic constant gives us a better ability to understand how the solid mechanical stability can change under the forces.

In this subsection, we have investigated the elastic constants and mechanical properties of the three Chalcogenide double perovskites Ca_2GaNbS_6, Sr_2GaNbS_6, and Ba_2GaNbS_6. The elastic constants have been acquired by means of calculating energy with regard to the tetragonal and rhombohedral pressure [38]. Thus, only the three independent elastic constants C_{11}, C_{12}, and C_{44} are needed for materials with cubic symmetry, which should satisfy the well-known Born stability criteria [39]. The Born stability criteria for cubic symmetry are: $C_{11} > 0$, $C_{44} > 0$, $C_{11} - C_{12} > 0$, $C_{11} + 2C_{12} > 0$ and $C_{12} < B < C_{11}$. The most important mechanical properties of compounds are the bulk modulus B, shear modulus G, have been determined by using the Voigt-Reuss-Hill approximations [40] with following formulas: $B_V = B_R = (C_{11} + 2C_{12})/3$, $B = (B_R + B_R)/2$, $G_V = (C_{11} - C_{12} + 3C_{44})/5$, $G_R = 5C_{44}(C_{11} - C_{12}) / (4C_{44} + 3C_{11} - C_{12})$, $G_V = (G_R + G_V)/2$, and Young's modulus E and Poisson's ratio ν via: $E = 9GB/3B + G$, $\nu = 3B - 2G/2(3B + G)$. Also, the Zener anisotropy factor is $A = 2C_{44}/(C_{11}+C_{12})$.

The calculated elastic constants and mechanical properties at (0 K, 0 GPa) for the three Chalcogenide double perovskite compounds A_2GaNbS_6 (A=Ca, Sr and Ba) are listed in Table II. From the Table the elastic constants C_{11}, C_{12}, and C_{44} are positive comply with Born stability criteria, which indicate that our compounds are mechanically stable in the cubic phase. Using these values to computed the others mechanical parameters. In the view of Table II, it can be understood that the obtained values of the bulk module B are in excellent agreement with those

of Table 1 (the optimized structural properties), which proves the reliability of the computed elastic properties. The rigidity of materials is affirmed after calculate Young's modulus (E), our low Young's modulus values tend to make the three Chalcogenide double perovskite compounds elastic and ductile. The ductility of materials is defined with: The value of Poisson's ratio (υ), Pugh's ratio (B/G), and Cauchy pressure ($C_P = C_{12}-C_{44}$) are greater than 0.26, 1.75, and 0, respectively [41], thereby our computed values of Poisson's ratio (υ), Pugh's ratio (B/G), and Cauchy pressure (in Table 2) indicate the ductile character of the three Chalcogenide double perovskite compounds A_2GaNbS_6 (A=Ca, Sr and Ba). For Zener's anisotropy factor A is equal to 1 for the isotropic materials, different value than 1 for the anisotropic materials [42], so our results are up above 1 which signify that our compounds have an anisotropic nature.

Another parameter has been calculated: the melting temperature T_m using the empiric expression $T_m(K) = [553\ (K) + (5.911)\ C_{11}]$ GPa ± 300 K [43], thereby the large values of T_m of the present materials indicate that A_2GaNbS_6 (A=Ca, Sr and Ba) can be maintain their crystal stability over a large range of temperatures. No experiment or theoretical data found for the elastic properties to compare with it.

Table 2. Elastic constants C11, C12, C44 (GPa), Bulk modulus B (GPa), Voigt Modulus G_R (GPa), Reuss Modulus G_R(GPa), Shear Modulus G (GPa), Young's modulus E (GPa), Poisson's ratio v, Pugh's ratio (B/G), Cauchy's pressure ($C_p = C_{12}-C_{44}$), Zener anisotropy factor A and melting temperature Tm (K).

Compound	C_{11}	C_{12}	C_{44}	B	G	E	υ	B/G	C_p	A	T_m
Ca_2GaNbS_6	96.2949	64.6467	28.7055	75.196	22.603	61.633	0.363	3.32	35.9412	1.81	1122.1028
Sr_2GaNbS_6	101.0334	59.5276	33.7754	73.362	27.782	74.004	0.331	2.64	25.7522	1.62	1150.1073
Ba_2GaNbS_6	110.1144	53.2715	38.0872	72.219	33.873	87.879	0.297	2.132	15.1843	1.32	1203.7761

3. 3. Electronic properties

To detect the electronic properties of the Chalcogenide A_2GaNbS_6 (A=Ca, Sr and Ba) double perovskites; at first, we have calculated the band structures using mBJ potential in the range of energy from -8 eV to 8 eV. In this work, E_f = 0 eV indicates the Fermi level. The calculated band structures are depicted in Figure 3.

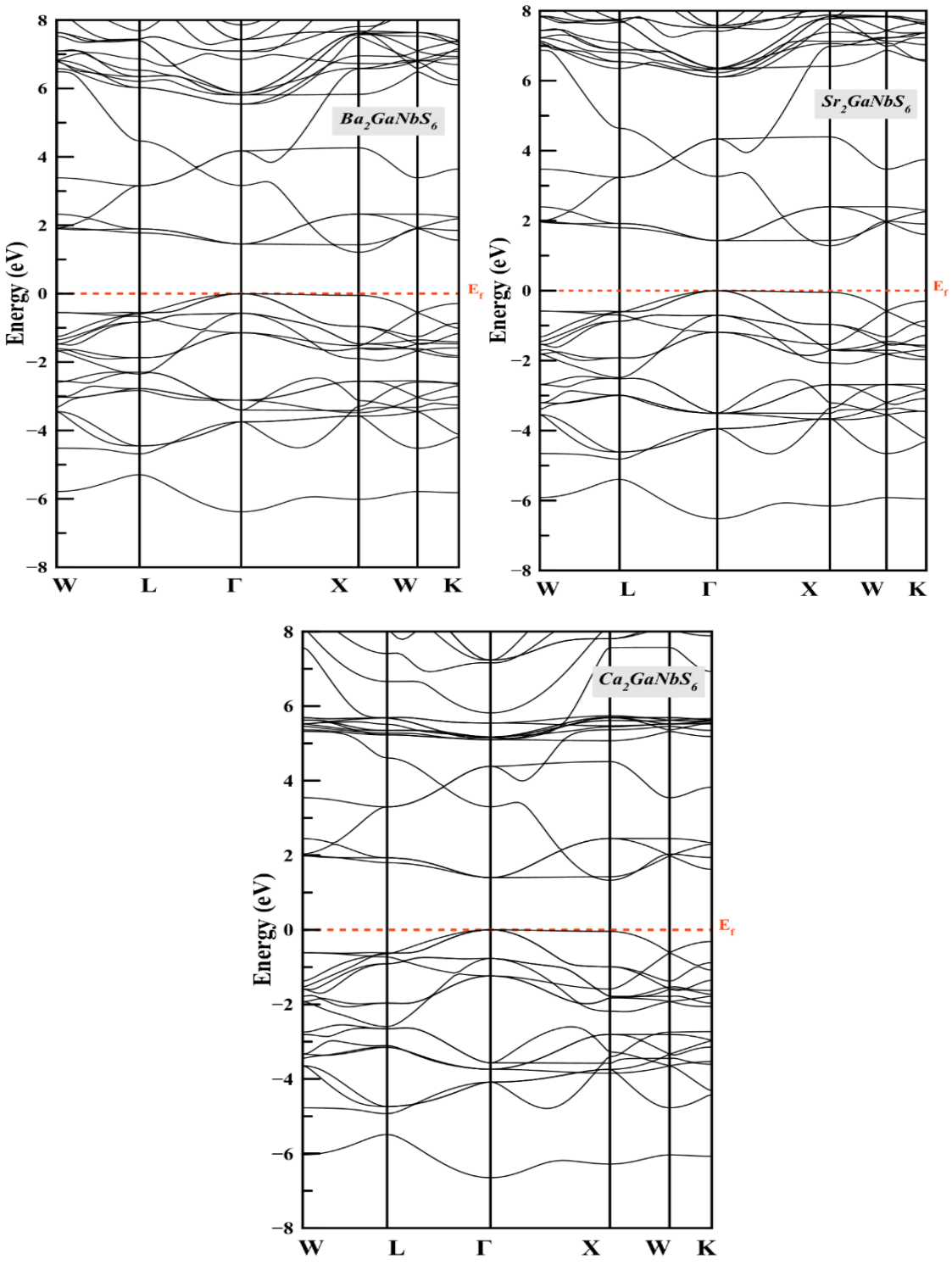


Figure 3. The band structure calculations of the three double perovskites Ba_2GaNbS_6, Sr_2GaNbS_6 and Ca_2GaNbS_6 compounds using mBJ potential.

The overall profiles of obtained band structures of the three compounds are almost similar. The chalcogenides Ba_2GaNbS_6, Sr_2GaNbS_6 and Ca_2GaNbS_6 have an indirect band gap of 1.21 eV, 1.28 eV and 1.32 eV, respectively, which is between the maximum of valence band (VBM) at Γ-point and the minimum of conduction band (CBM) at X-point. But it can be cited that the three compounds have a pseudo-direct gaps with difference of ~0.045eV with indirect ones at the same X-point for the VBM and CBM. These features are listed in Table 3. According to our knowledge, no experimental results have been reported in scientific literature.

Table 3. Calculated fundamental energy band gap E_g in eV of the double perovskites A_2GaNbS_6 (Ca, Sr and Ba)

Compounds	**Ba_2GaNbS_6**	**Sr_2GaNbS_6**	**Ca_2GaNbS_6**
Direct $X - X$	1.2613[a]	1.3308[a]	1.3728[a]
Indirect $\Gamma - X$	1.2109[a] 1.19[b]	1.2844[a] -	1.3295[a] 1.19[b]

[a]mBJ, this work. [b]Other theoretical work, Ref [28].

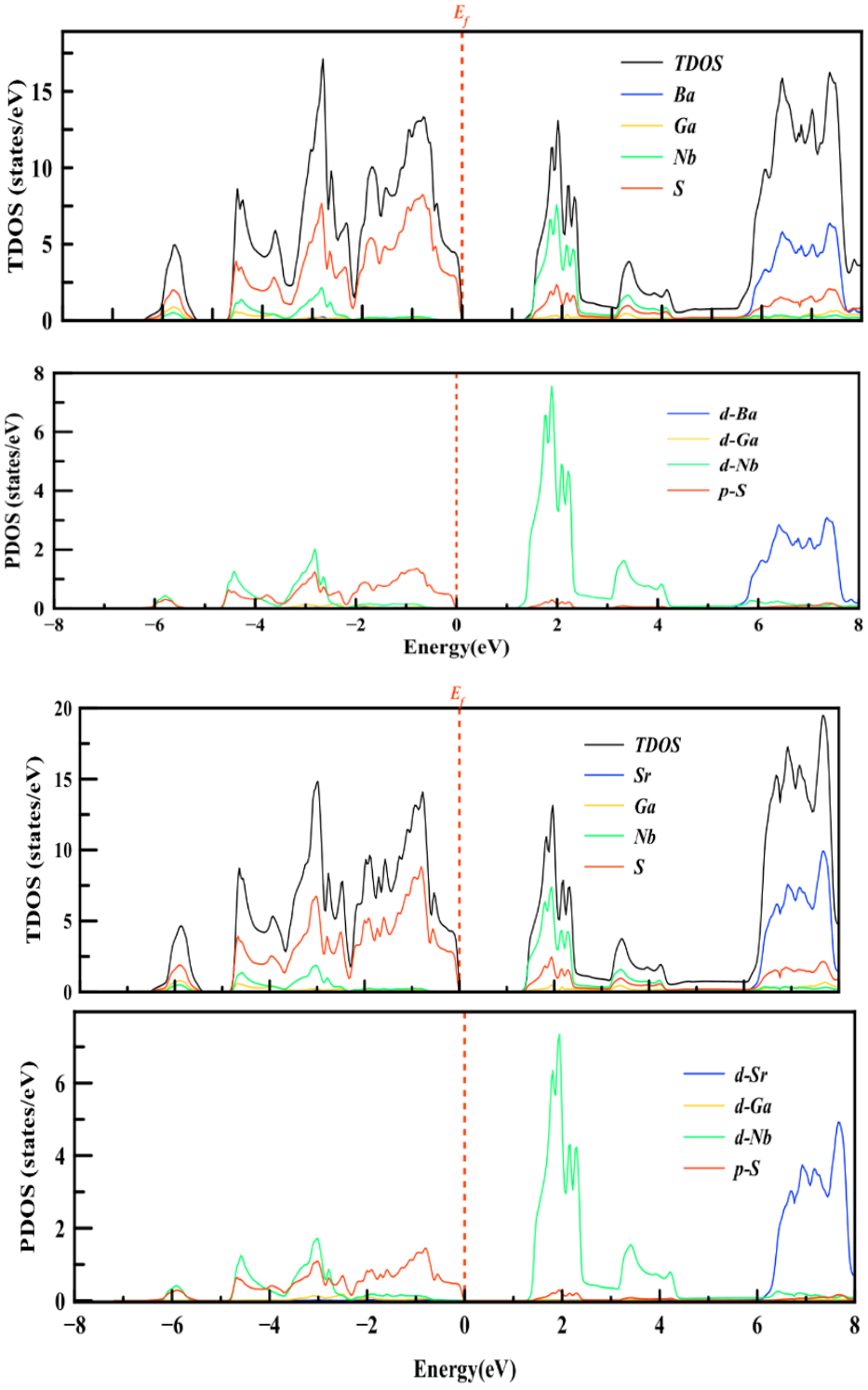
A further examination of electronic structure can be achieved by calculating the density of states (total and partial) using mBJ potential, the plots of the total and partial density of states for examined compounds Ba_2GaNbS_6, Sr_2GaNbS_6 and Ca_2GaNbS_6 are shown in Fig. 4 for energy in the range of -8 eV to 8 eV. From the figure, the valence band (VB) is produced after the hybridization between the S-3p states and the Nb-4d states at [-6.22 eV- 0 eV] for Ba_2GaNbS_6, [-6.38 eV - 0 eV] for Sr_2GaNbS_6, [-6.59 eV -0 eV] for Ca_2GaNbS_6) and it is observed that the increased spread energy of the uppermost part of the valence band is attributed to the increases in the size of the atoms from Ba to Ca, while the conduction band (E≥ Ef=0 eV) is composed of the Nb-4d states with little contribution from the S-3p states and the top of conduction band formed principally of A-d (Ba-5d, Sr-4d and Ca-3d) states, in all cases.

3. 4. Optical properties

The optical properties such as reflectivity, absorption coefficient, refractive index, and optical conductivity of a compound can be obtained by studying the complex dielectric function ε (ω) using the Ehrenreich and Cohen's equation [44]:

$$\varepsilon(\omega) = \varepsilon_1(\omega) + i\varepsilon_2(\omega) \quad (2)$$

where $\varepsilon_1(\omega)$ the real part and $\varepsilon_2(\omega)$ imaginary part can be determined independently. However, $\varepsilon_2(\omega)$ directly from the electronic structure and $\varepsilon_1(\omega)$ from Kramers-kroing relation [45]; these two parts represent the electronic polarizability under incident light and absorption behavior [46].



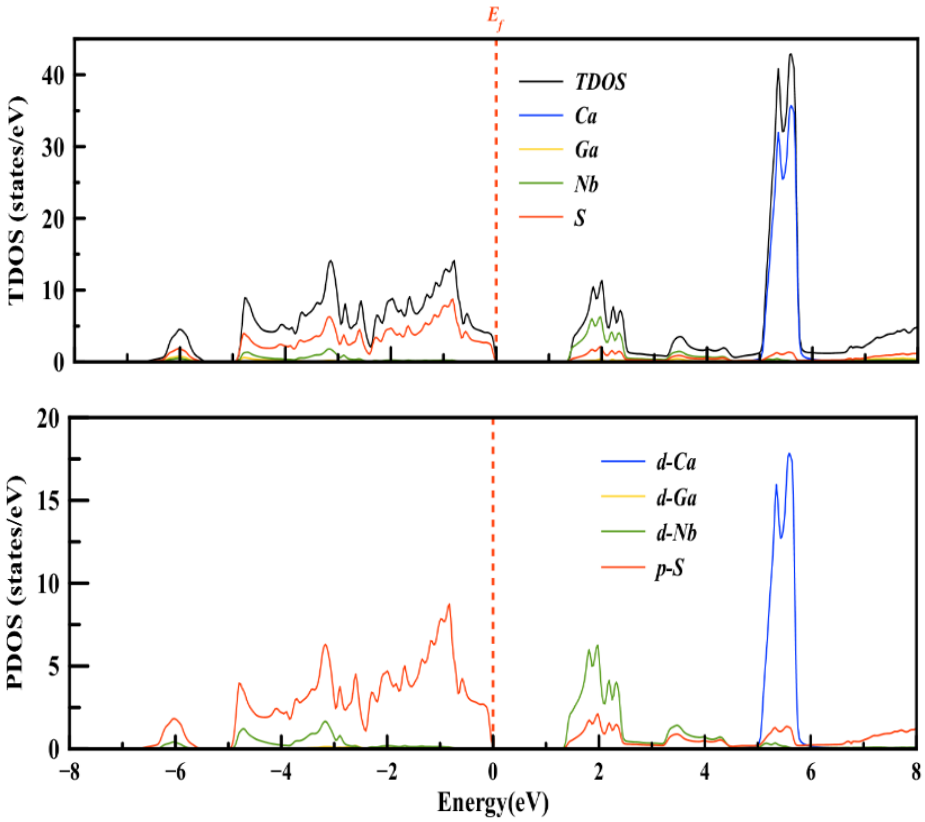


Figure 4. Total and partial density of states (TDOS /PDOS) for the double perovskites Ba_2GaNbS_6, Sr_2GaNbS_6 and Ca_2GaNbS_6 using mBJ potential.

In this part, we have evaluated the optical responses of the chalcogenide A_2GaNbS_6 (A=Ca, Sr and Ba) double perovskites in a large energy range (>34 eV). The Fig. 5a represent the evolution of the real ε_1 (ω) of the dielectric function ε (ω) for the three chalcogenide double perovskite compounds. At zero frequency limit, the static dielectric constant ε_1 (0) is 6.936, 6.959 and 7.223 for Ca_2GaNbS_6, Sr_2GaNbS_6 and Ba_2GaNbS_6, respectively. Note that the value of ε_1 (0) increases with the decrease of band gap (E_g (Ba)< E_g (Sr) < E_g (Ca)). The inverse relation between ε_1 (0) and E_g, which agrees with Penn's model:

$$\varepsilon_1(0) \approx 1 + \frac{\hbar\omega_p}{E_g} \qquad (3)$$

Where ω_p plasma frequency and E_g energy band gap. For the three cases, ε_1 (ω) appear the growing tendency to achieve its maximum of 13.290 at 2.272 eV for Ca_2GaNbS_6, of 13.532 at 2.326 eV for Sr_2GaNbS_6 and 13.141 at 2.217 eV for Ba_2GaNbS_6. After then we notice the decreasing of the curves until they attain the negative values from 11.170 eV to 11.578 eV and 18.571 eV to 23.388 eV for Ba_2GaNbS_6 compound, from 11.197 eV to 18.082 eV and 24.939

eV to 26.190 eV for Sr_2GaNbS_6 compound and 10.898 eV to 19.088 eV and 29.238eV to 30.327 eV for Ca_2GaNbS_6 compound.

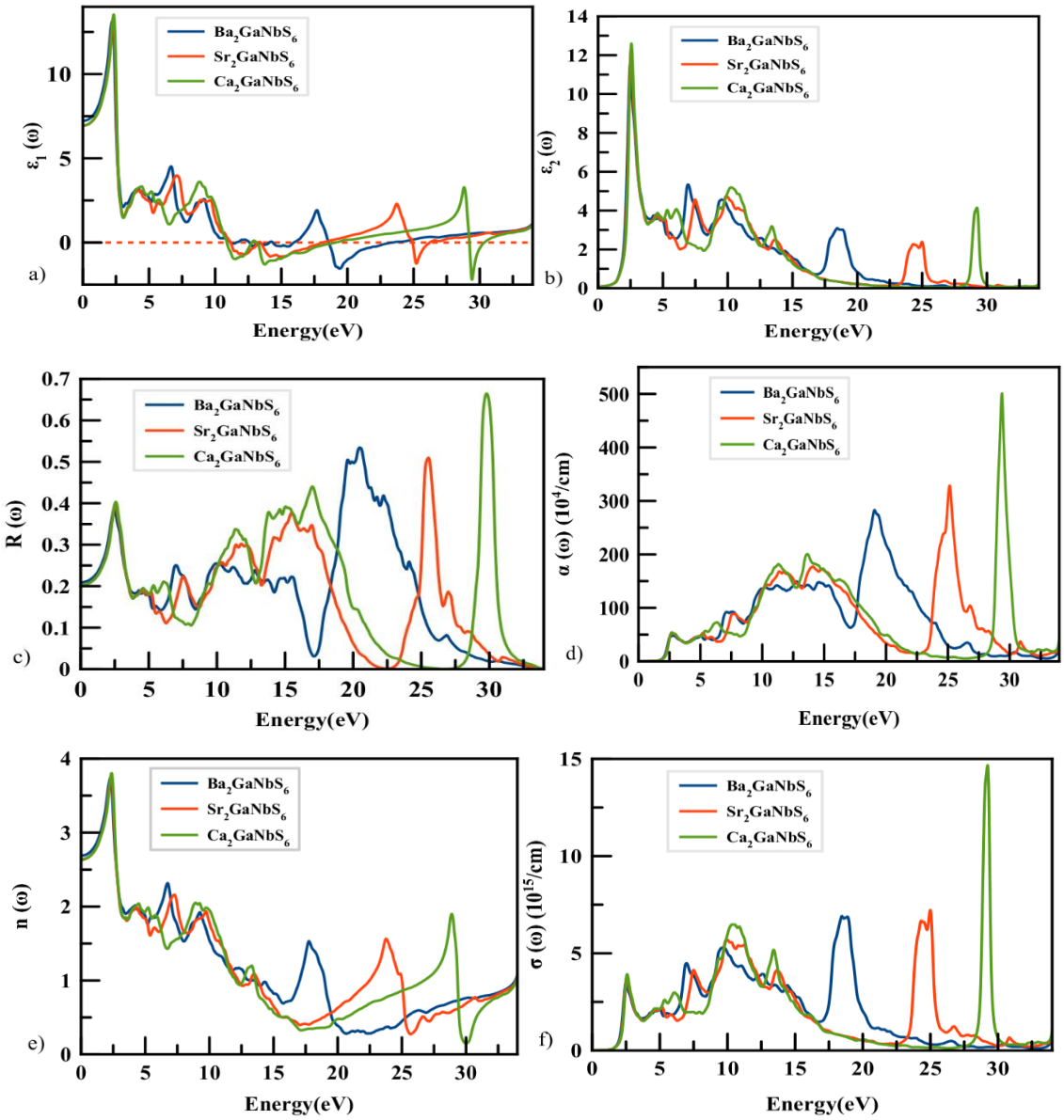


Figure 5. Calculated: a) Real ε_1 (ω) and b) Imaginary part ε_2 (ω) of complex dielectric function; c) Reflectivity R (ω), d) Absorption coefficient α (ω), e) Refraction index n (ω) and f) Optical conductivity σ(ω).

The negative values of $\varepsilon_1(\omega)$ imply that light is completely attenuated in the optical medium. Hence, in this energy range; where $\varepsilon_1(\omega)$ is negative, incident electromagnetic waves are completely reflected and the material loses its dielectric properties. The Fig .5b shows the imaginary part ε_2 (ω) of the dielectric function ε (ω). It is observed that the maximum value of ε_2 (ω) is 12.597 at 2.571 eV for Ca_2GaNbS_6, 12.251 at 2.544 eV for Sr_2GaNbS_6 and 11.494 at 2.489 eV for Ba_2GaNbS_6 compound, which mean ε_2 (ω) takes values from the band gap calculations. As illustrated in Fig.5c, the zero-frequency reflectivity R (0), that is the static part

of reflectivity R(ω) is at 20.22%, 20.28 % and 20.94% for Ca_2GaNbS_6, Sr_2GaNbS_6 and Ba_2GaNbS_6 compounds, respectively. Furthermore, the maximum dynamic reflectivity is 53.39% at 20.51 eV for Ba_2GaNbS_6, 50.83% at 25.56 eV for Sr_2GaNbS_6 and 66.33% at 29.75 eV for Ca_2GaNbS_6 compound. Additionally, the maximum reflectivity R(ω) set at the energy variety from 20 eV to 30 eV, in a similar way for the negative value of $\varepsilon_1(\omega)$ for the three compounds, which this variation of the reflectivity magnitude with energy is appropriate for Bragg's reflector [47]. Fig.5d represents the absorption coefficient in the function of the energy of the chalcogenide A_2GaNbS_6 (A=Ca, Sr and Ba) compounds. Of the figure, the three investigated materials have two separated absorption bands in the studied energy range. The first begins from their particular band gap (the visible range) and diffuses up to about 13 eV, whilst the second one is established at 29.374eV, 25.129 eV and 19.069 eV for Ca_2GaNbS_6, Sr_2GaNbS_6 and Ba_2GaNbS_6 (ultraviolet range), respectively.

The calculated frequency-dependent refractive index n (ω) of the three materials is depicted in Fig. 5e. The obtained static refractive index n (0) from the static dielectric constant by the equation: $n(0) = \sqrt{\varepsilon_1(0)}$ .It equal to 2.634, 2.638 and 2.687 for Ca_2GaNbS_6, Sr_2GaNbS_6 and Ba_2GaNbS_6, respectively. Also, its remarkable that n(ω) increases with increasing energy, reaching its maximum value of 3.735 at 2.272 eV for Ba_2GaNbS_6, 3.771 at 2.353 eV for Sr_2GaNbS_6 and 3.803 at 2.381 eV for Ca_2GaNbS_6 compound. These peaks are found at the lowest energy, which may be due to the decrease of band gap as E_g (Ba)< E_g (Sr) < E_g (Ca). Fig 5f. shows the optical conductivity σ (ω) of the three compounds. We perceived that the optical conductivity is identically aspect with absorption coefficient.6.845 (10^{15}/cm) for Ba_2GaNbS_6,7.162(10^{15}/cm) for Sr_2GaNbS_6 and 14.651(10^{15}/cm) for Ca_2GaNbS_6 are the maximum optical conductivity values at high energies of 18.789 eV, 25.021 eV and 29.211 eV, respectively.

The chalcogenide A_2GaNbS_6 (A=Ca, Sr and Ba) double perovskites are especially promising for optoelectronic devices in the visible and ultraviolet energy ranges since they are indirect gap materials that possess properties of a direct band gaps materials, like the optimal value for an absorber in a single junction solar cell.

3. 5. Thermoelectric properties

In this section, we are calculated from the electronic band structure obtained with mBJ potential the thermoelectric properties (TE) of the chalcogenide A_2GaNbS_6 (Ca, Sr and Ba) double perovskites which include Seebeck coefficient S, thermopower factor PF, electrical

conductivity σ, electronic thermal conductivity k_e, and figure of merit ZT using the semiclassical Boltzmann equation solved under constant relaxation time approximation $\tau = 1.0 \times 10^{-15}$ s, as embedded in BoltzTrap code [33] (with all of details of the method in Ref [48]).Therefore, the *k*-point mesh is increased to 150000 for better convergence and a suitable range of temperature from 200 K to 1200 K to acquire precise transport coefficients.

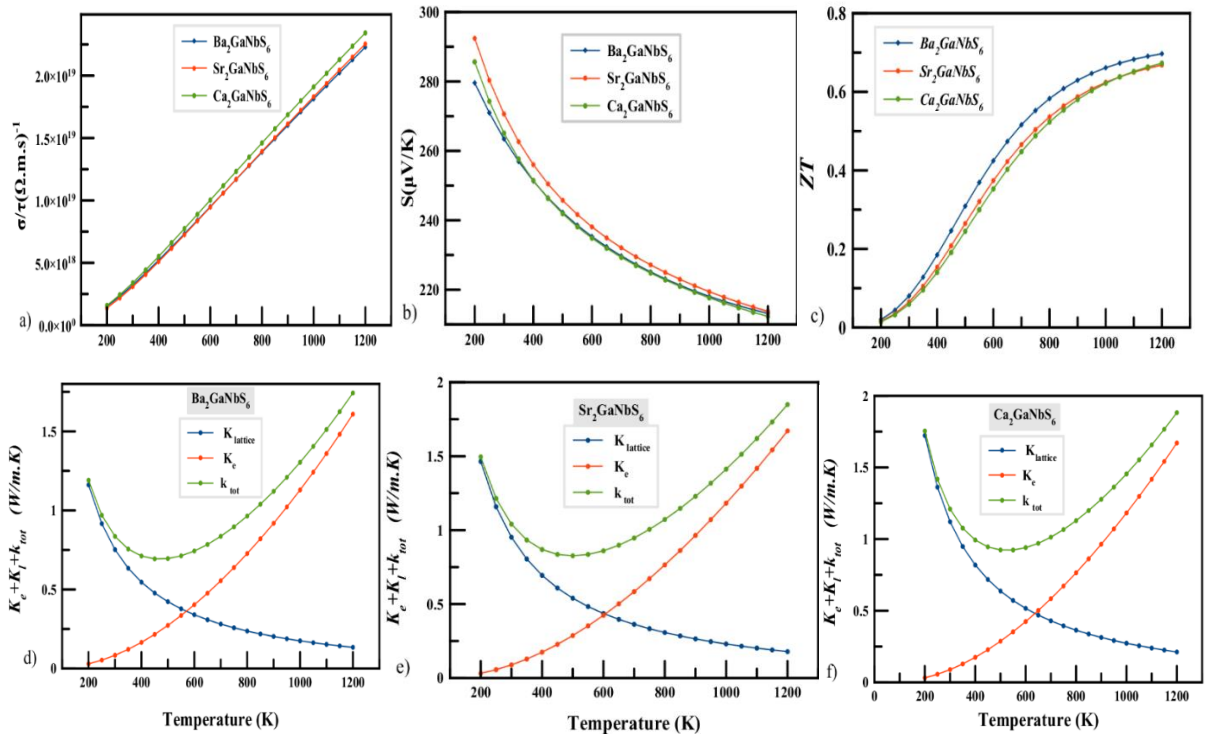


Figure 6. Calculated thermoelectric properties of the double perovskite compounds A_2GaNbS_6 (Ca, Sr and Ba): a) Electrical conductivity; b) Seebeck coefficient; c) Figure of merit; d) e) f) Electronic thermal conductivity k_e, lattice thermal conductivity k_L, total thermal conductivity K_{tot}.

In Fig. 6a, the variation of the electrical conductivity σ/τ as a function of the temperature for the A_2GaNbS_6 (Ca, Sr and Ba) double perovskites is plotted, we can observe that the electrical conductivity (σ/τ) increases with increasing temperature from 1.52×10^{18} $(\Omega ms)^{-1}$ at 200 K for the three compounds until reaching a maximum value of 2.34×10^{19}, 2.25×10^{19} and 2.22×10^{19} Ωms^{-1} at 1200 K for Ca_2GaNbS_6, Sr_2GaNbS_6 and Ba_2GaNbS_6, respectively. The variation of Seebeck coefficient (*S*) against temperature for the A_2GaNbS_6 (Ca, Sr and Ba) double perovskites is displayed in Fig. 6b. This figure shows that the Seebeck coefficient (*S*) for the three compounds decreases with an increase in temperature of 292.42 μV/K at 200 K to 213.74 μV/K at 1200 K for Sr_2GaNbS_6, of 279.59 μV/K at 200K to 213.17 μV/K at 1200 K for Ba_2GaNbS_6 and 285.6 μV/K at 200K to 212.29 μV/K at 1200 K for Ca_2GaNbS_6.

Figures 6. d-f represent the total thermal conductivity ($K_{tot} = k_e + k_L$) dependence on temperature, the lattice thermal conductivity k_L, and the electronic thermal conductivity k_e

contributions. The lattice thermal conductivity was determined after Slack's equation [49]. The figures are clearly shows the electronic thermal conductivity k_e is increasing with increasing temperature occurs from 0.029 to 1.609 W/mK, 0.0314 to 1.670 W/mK and 0.0315 to 1.670 W/mK for Ba_2GaNbS_6, Sr_2GaNbS_6 and Ca_2GaNbS_6 compounds, respectively. while the lattice part k_L decreases with an increase in temperature from 1.161 to 0.133 W/mK, 1.464 to 0.178 W/mK and 1.722 to 0.211W/mK for Ba_2GaNbS_6, Sr_2GaNbS_6 and Ca_2GaNbS_6 compounds, respectively. The total thermal conductivity k_{tot} shows an exponential decaying trend in all compounds up to 600 K due to the abrupt increase of large phonon vibrations slightly with increases temperature.

The TE ability of three A_2GaNbS_6 (A=Ca, Sr and Ba) double perovskites is explored through the determination of the figure of merit (ZT). Here we have plotted the variation of ZT against the temperature in Fig. 6c, which shows linearly that ZT increase with increasing temperature from the minimum values of 0.02, 0.015 and 0.014 at 200 K to the maximum values of 0.697, 0.668 and 0.672 at 1200K. The obtained results from the Ab-initio calculations reveal that the chalcogenide A_2GaNbS_6 (Ca, Sr and Ba) double perovskites compounds are promising thermoelectric materials.

4. Conclusion

In summary, we carried out a detailed study of structural, electronic, elastic, optical, and thermoelectric properties of chalcogenide A_2GaNbS_6 (Ca, Sr and Ba) double perovskites using ab initio calculations, with FP-LAPW method implemented in Wien2k code. GGA and mBJ potential were used for exchange-correlation. The structural computations signify the stability of non-magnetic A_2GaNbS_6 (A=Ca, Sr and Ba) in the cubic (Fm-3m) configuration. The electronic profile analyzed from the Band Structure and density of states plots exhibits the semiconducting character with an indirect band gap. The chalcogenide A_2GaNbS_6 (Ca, Sr and Ba) double perovskites are especially promising for optoelectronic devices since they are indirect gap materials that possess the properties of direct band gap materials because of the wide absorption bands and high reflectivity in a wide energy range from visible to ultraviolet. Calculated thermoelectric properties which include electrical conductivity, electronic thermal conductivity, lattice thermal conductivity, and Seebeck coefficient after the semi-classical Boltzmann transport theory reveal that the chalcogenide A_2GaNbS_6 (A= Ca, Sr and Ba) double perovskites are a promising thermoelectric material. To our knowledge, no other studies of physical properties are available in the literature for these materials; thus, it would be beneficial to verify experimentally our predicted results.

Acknowledgments

The research was supported by the General Division for Algerian scientific Research and technological development (DGRSTD). https://www.mesrs.dz/dgrsdt.

References

[1] M. Grätzel, “Solar Energy Conversion by Dye-Sensitized Photovoltaic Cells”. *Inorg. Chem.* (2005), 44, 20, 6841–6851.

[2] T. M. Tritt and M.A. Subramanian, MRS Bulletin, “Thermoelectric Materials, Phenomena, and Applications: A Bird's Eye View”. (2006),31, 188

[3] D. Kraemer, L. Hu, A. Muto, X. Chen, G. Chen, and M. Chiesa, "Photovoltaic-thermoelectric hybrid systems: A general optimization methodology", *Appl. Phys. Lett*. (2008), 92, 243503.

[4] Jung, H.S. and Park, N. “Perovskite Solar Cells: From Materials to Devices”. *Small*. (2015), 11, 10-25.

[5] M. Rull-Bravo, A. Moure, J. F. Fernandez and M. Martin-Gonzalez, “Skutterudites as thermoelectric materials: revisited”. *RSC Adv*, 5, (2015) 41653.

[6] Vikram, J. Kangsabanik, Enamullah and A. Aftab, “Bismuth based half-Heusler alloys with giant thermoelectric figures of merit”. *J. Mater. Chem. A*.5 (2017) 6131-6139

[7] M. Khetir, A. Maafa, F. Boukabrine, H. Rozale. A. Bouab ,and A. Chahed, “Elastic constants, electronic properties and thermoelectric response of LiAIX (X=C, Si, Ge, and Sn) half-Heusler compounds”, *Rev Mex Fisica*. 68 (2022) 011002.

[8] M. Grätzel, “The light and shade of perovskite solar cells”. *Nat Mater.*13, (2014) 838-842.

[9] C. Liu, J. Fan, X. Zhang, Y. Shen, L. Yang and Y. Mai, “Hysteretic Behavior upon Light Soaking in Perovskite Solar Cells Prepared via Modified Vapor-Assisted Solution Process”. *ACS Appl Mater Interfaces*. 17 (2015) 9066-9071.

[10] HS. Kim, JY. Seo, NG. Park, “Material and Device Stability in Perovskite Solar Cells”. *ChemSusChem*. 18, (2016) 2528-2540.

[11] M. Ullah, S. A. Khan, G. Murtaza, R. Khenata, N. Ullah, S. Bin Omran, Electronic, thermoelectric and magnetic properties of La_2NiMnO_6 and La_2CoMnO_6, *Journal of Magnetism and MagneticMaterials.*377, (2015)197-203.

[12] Babayigit, A., Ethirajan, A., Muller, M. et al. “Toxicity of organometal halide perovskite solar cells”. *Nature Mater (*2016) 15, 247–251.

[13] S. Meenakshi, V. Vijayakumar, S.N. Achary, A.K. Tyagi, "High pressure investigation on double perovskite Ba2MgWO6", *Journal of Physics and Chemistry of Solids*, 72, (2011), 609-612.

[14] A.W. Sleight and R. Ward, "Compounds of Heptavalent Rhenium with the Perovskite Structure", *J. Am. Chem. Soc*. 83, 5, (1961)1088–1090.

[15] F.K. Patterson, Ca.W. Moeller, and R. Ward, "Magnetic Oxides of Molybdenum(V) and Tungsten(V) with the Ordered Perovskite Structure", *Inorg. Chem*. 2, 1, (1963) 196–198.

[16] F. S. Galasso, F. C. Douglas, and R. J. Kasper, "Relationship Between Magnetic Curie Points and Cell Sizes of Solid Solutions with the Ordered Perovskite Structure", *J. Chem. Phys*. 44, (1966)1672

[17] M. T. Anderson, K. B. Greenwood, G. A. Taylor and K. R. Poeppelmeier, "B-Cation Arrangements in Double Perovskites", *Progress in Solid State Chemistry*, 22, 3, (1993) 197-233.

[18] K. Ramesha, V. Thangadurai, D. Sutar, S. Subramanyam, G.N. Subbanna, J. Gopalakrishnan, "ALaMnBO6 (A=Ca, Sr, Ba; B=Fe, Ru) double perovskites", *Materials Research Bulletin*,35, (2000)559-565.

[19] J. B. Philipp, P. Majewski, L. Alff, A. Erb, R. Gross, *et al* "Structural and doping effects in the half-metallic double perovskite A2CrWO6 (A=Sr, Ba, and Ca)", *Phys. Rev. B*,68, (2003)144431.

[20] Al. Dutta, T. P. Sinha, and S. Shannigrahi, "Dielectric relaxation and electronic structure of double perovskite Sr2FeSbO6," *Journal of Applied Physics*,104, (2008) 064114.

[21] H.-R. Fuh, K.-C. Weng, Y.-P. Liu, Y.-K. Wang, J. "New ferromagnetic semiconductor double perovskites: La2FeMO6 (M = Co, Rh, and Ir) ". *Alloys Compd*. 622 (2015) 657–661.

[22] N. Zu, J. Wang, Y. Wang, Z. Wu, J. "Half metallicity in Sr2CrOsO6 via Na doping". *Alloys Compd*. 636 (2015) 257–260.

[23] S. Zhao, C. Lan, J. Ma, S.S. Pandey, S. Hayase, T. Ma, "Research Update: Behind the high efficiency of hybrid perovskite solar cells. "*Solid State Commun*. 213214 (2015) 19–23.

[24] L. Agiorgousis, Y. Sun, D-H. Choe, D. West and S. Zhang." Machine Learning Augmented Discovery of Chalcogenide Double Perovskites for Photovoltaics". *Adv. Theory Simul*. 2, (2019)1800173.

[25] W. Kohn and L. J. Sham, "Self-Consistent Equations Including Exchange and Correlation Effects", *Phys. Rev.* 140, (1965) A1133.

[26] M. C. Payne, M. P. Teter, D. C. Allan, T. A. Arias, and J. D. Joannopoulos," Iterative minimization techniques for ab initio total-Energy calculations: molecular dynamics and conjugate gradients", *Rev. Mod. Phys*. 64, (1992) 1045.

[27] P. Blaha, K. Schwarz, F. Tran, R. Laskowski, G. K. H. Madsen, and L.D. Marks, "WIEN2k: An APW+lo program for calculating the properties of solids", J. Chem. *Phys.* 152, (2020) 074101.

[28] U.V. Barth and L. Hedin, "A local exchange-correlation potential for the spin polarized case. i", *J. Phys. C: Solid State Phys*.5, (1972)1629.

[29] J. P. Perdew, K. Burke, and M. Ernzerhof, "Generalized Gradient Approximation Made Simple", *Phys. Rev. Lett*. 78, (1997)1396.

[30] A. R. Jishi, B. Oliver and A. Sharif, "Modeling of Lead Halide Perovskites for Photovoltaic Applications", *J. Phys. Chem. C,* 118, (2021)28344-28349.

[31] H. J. Monkhorst and J. D. Pack, "Special points for Brillouin-zone integrations", *Phys. Rev. B*. 13, (1976) 5188.

[32] D. Becke and M. R. Roussel, "Exchange holes in inhomogeneous systems: A coordinate-space model", *Phys. Rev.* 39, (1989) 3761.

[33] G. K. H. Madsen, and D. J. Singh, BoltzTraP. A code for calculating band-structure dependent quantities. Comput. *Phys. Commun*.,175(2006)67.

[34] A. E. Fedorovskiy, N. A. Drigo, M.K. Nazeeruddin, "The role of Goldschmidt's tolerance factor in the formation of A_2BX_6 double halide perovskites and its optimal range", *Small Methods* (2019) 1900426–1900432.

[35] S. A. Khandy and D. C. Gupta, "Magneto-electronic, Mechanical, Thermoelectric and Thermodynamic Properties of Ductile Perovskite Ba2SmNbO6". *Mater. Chem. Phys*., 239, (2020)121983.

[36] Wyckoff, W. G. Ralph, The analytical expression of the results of the theory of space-groups, Carnegie Institute of Washington, Washington, 318.

[37] V. G. Tyuterev and N. Vast, "Murnaghan's Equation of State for the Electronic Ground State Energy," Computational Materials Science, (2006),350353.

[38] M. J. Mehl, J. E. Osburn, D. A. Papaconstantopoulos, and B. M. Klein, "Structural properties of ordered high-melting- temperature intermetallic alloys from first-principles total- energy calculations". *Phy. Rev. B,* 41 (1990) 10311.

[39] M. Born, "In on the Stability of Crystal Lattices". *Cambridge University Press*, 1940, p. 160.

[40] M. Dacorogna, J.s. Ashkenazi, M. Peter, “Ab initio calculation of the tetragonal shear moduli of the cubic transition metals”, *Phy. Rev. B.*26 (1982) 1527.

[41] Seh AQ, Gupta DC. “Exploration of highly correlated co- based quaternary Heusler alloys for spintronics and thermoelectric applications”. *Int J Energy Res*.43 (2019) 8864- 8877.

[42] B. Benichou, Z. Nabi, B. Bouabdallah, H. Bouchenafa. “Ab initio investigation of the electronic structure, elastic and magnetic properties of quaternary Heusler alloy Cu2MnSn1−xInx (x = 0, 0.25, 0.5, 0.75, 1)”. *Rev Mex Fis* 64, (2018) 135.

[43] M. E. Fine, L. D. Brown, and H. L. Marcus, “Elastic constants versus melting temperature in metals*”. Scr. Mettal*, 18 (1984) 951.

[44] H. Ehrenreich and M. H. Cohen, “Self-Consistent Field Approach to the Many-Electron Problem”, *Phys. Rev*. 115, (1959) 786.

[45] John S. Toll, “Causality and the Dispersion Relation: Logical Foundations”, *Phys. Rev.* 104, (1956) 1760-1770.

[46] R. M. A. Azzam and A. M. El-Saba, “Reflectance of an absorbing substrate for incident light of arbitrary polarization: appearance of a secondary maximum at oblique incidence”, Appl.*Opt*.27,(1988)4034-4037.

[47] B. Amin, I. Ahmad, M. Maqbool, S. Goumri-Said and R. Ahmad, “Ab initio study of the bandgap engineering of $Al_{1-x}Ga_xN$ for optoelectronic applications”, *Journal of Applied Physics*,109, (20113) 023109.

[48] G. Madsen,D. J.Singh, BoltzTraP. “A code for calculating band-structure dependent quantities”, *Computer Physics Communications*,175, (2006) 67-71.

[49] G. A. Slack, “Nonmetallic crystals with high thermal conductivity”, *J. Phys. Chem. Solids*, 34 (1973) 321.